

PREPARED FOR THE U.S. DEPARTMENT OF ENERGY,
UNDER CONTRACT DE-AC02-76CH03073

PPPL-3918
UC-70

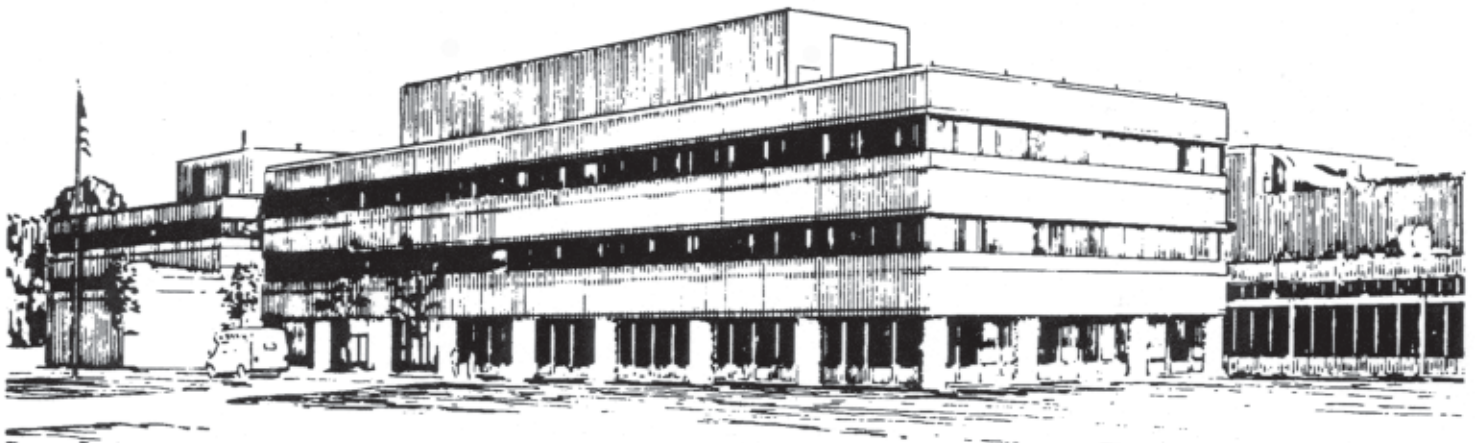
PPPL-3918

**Measurement of the Magnetic Field in a Spherical Torus Plasma
via Electron Bernstein Wave Emission Harmonic Overlap**

by

B. Jones, G. Taylor, P.C. Efthimion, and T. Munsat

January 2004



**PRINCETON PLASMA PHYSICS LABORATORY
PRINCETON UNIVERSITY, PRINCETON, NEW JERSEY**

PPPL Reports Disclaimer

This report was prepared as an account of work sponsored by an agency of the United States Government. Neither the United States Government nor any agency thereof, nor any of their employees, makes any warranty, express or implied, or assumes any legal liability or responsibility for the accuracy, completeness, or usefulness of any information, apparatus, product, or process disclosed, or represents that its use would not infringe privately owned rights. Reference herein to any specific commercial product, process, or service by trade name, trademark, manufacturer, or otherwise, does not necessarily constitute or imply its endorsement, recommendation, or favoring by the United States Government or any agency thereof. The views and opinions of authors expressed herein do not necessarily state or reflect those of the United States Government or any agency thereof.

Availability

This report is posted on the U.S. Department of Energy's Princeton Plasma Physics Laboratory Publications and Reports web site in Fiscal Year 2004. The home page for PPPL Reports and Publications is: http://www.pppl.gov/pub_report/

DOE and DOE Contractors can obtain copies of this report from:

U.S. Department of Energy
Office of Scientific and Technical Information
DOE Technical Information Services (DTIS)
P.O. Box 62
Oak Ridge, TN 37831

Telephone: (865) 576-8401

Fax: (865) 576-5728

Email: reports@adonis.osti.gov

This report is available to the general public from:

National Technical Information Service
U.S. Department of Commerce
5285 Port Royal Road
Springfield, VA 22161

Telephone: 1-800-553-6847 or
(703) 605-6000

Fax: (703) 321-8547

Internet: <http://www.ntis.gov/ordering.htm>

Measurement of the magnetic field in a spherical torus plasma via electron Bernstein wave emission harmonic overlap

B. Jones^{a)}, G. Taylor, P.C. Efthimion, and T. Munsat

Princeton Plasma Physics Laboratory, Princeton University, Princeton, New Jersey 08543

Measurement of the magnetic field in a spherical torus by observation of harmonic overlap frequencies in the electron Bernstein wave (EBW) spectrum has been previously suggested [V.F. Shevchenko, Plasma Phys. Reports **26**, 1000 (2000)]. EBW mode conversion to X-mode radiation has been studied in the Current Drive Experiment-Upgrade spherical torus, [T. Jones, Ph.D. thesis, Princeton University, 1995] with emission measured at blackbody levels [B. Jones *et al.*, Phys. Rev. Lett. **90**, 165001 (2003)]. Sharp transitions in the thermally emitted EBW spectrum have been observed for the first two harmonic overlaps. These transition frequencies are determined by the magnetic field and electron density at the mode conversion layer in accordance with hot-plasma wave theory. Prospects of extending this measurement to higher harmonics, necessary in order to determine the magnetic field profile, and high- β equilibria are discussed for this proposed magnetic field diagnostic.

^{a)}Present Address: *Sandia National Laboratories, PO Box 5800, Albuquerque, New Mexico 87185-1168*; Electronic mail: bmjones@sandia.gov

I. INTRODUCTION

In many contemporary high- β magnetically confined fusion plasma devices, the plasma is “overdense” in that the plasma frequency (f_{pe}) is much greater than the first several harmonics of the electron cyclotron frequency (f_{ce}). In this regime, traditional electron cyclotron emission (ECE), heating and current drive techniques [1] cannot be applied in the same way as in conventional tokamaks. The electrostatic electron Bernstein wave (EBW) does propagate in overdense plasma, though, and is strongly absorbed at f_{ce} harmonic resonances [2,3]. As a result, electron temperature (T_e) diagnosis as well as heating and current drive via the EBW have been proposed for overdense plasma geometries including the spherical torus (ST), reversed field pinch (RFP), and stellarator.

While the EBW cannot propagate outside the plasma, it can be accessed via mode conversion to X-mode (B-X process) [4] or O-mode electromagnetic waves via the slow X-mode (B-X-O) [5]. Thermal emission has been observed via B-X conversion in Current Drive Experiment Upgrade (CDX-U) [6] and National Spherical Torus Experiment (NSTX) [7], as well as in the Madison Symmetric Torus RFP [8]. T_e profiles have been measured via B-X-O conversion in the Wendelstein 7-AS stellarator, [9] and heating experiments have also been performed via the inverse O-X-B process. [10]

In this paper, we discuss a previously proposed technique by which magnetic field profile information can be obtained in an ST by observation of harmonic overlaps in the EBW emission spectrum [11]. Harmonic overlaps occur at coincidences of the upper-hybrid and electron cyclotron harmonic frequencies, and are thus determined by the magnetic field (B) and electron density (n_e) profiles in the plasma. Sharp drops in the EBW emission spectrum occur at these

harmonic overlap frequencies, and by measuring these transitions either $B(R)$ or $n_e(R)$ can be determined from knowledge of the other profile. Reference 11 proposes the technique for B-X-O mode converted emission, and the same scheme is possible using the B-X converted radiation temperature (T_{rad}) as will be discussed. We present data from an experiment performed in the CDX-U ST in which the first two harmonic overlap frequencies are observed and found to agree with theoretical predictions using $n_e(R)$ measured with Langmuir probes and $B(R)$ modeled with the EFIT equilibrium code [12]. This work supports the validity of the diagnostic technique of Ref. 11, as well as the hot plasma wave theory [13] that predicts the EBW physics observed.

In section II, we discuss the physical origin of discrete transition frequencies in the mode-converted EBW emission spectrum. Section III describes the instrument employed in CDX-U to measure the EBW spectrum, and experimental measurements of the first two harmonic transitions are presented in section IV. In section V, the implementation of a magnetic field profile diagnostic based on this technique is discussed, along with the effect of high- β on the EBW spectrum. Finally, the results and conclusions are summarized in section VI.

II. HARMONIC OVERLAP IN THE EMITTED EBW SPECTRUM

Figure 1 shows the characteristic frequencies relevant to EBW emission and B-X mode conversion for nominal CDX-U plasma parameters ($R_0=34$ cm, $R_0/a\sim 1.5$, $B_{T0}=0.21$ T, $n_{e0}\sim 4\times 10^{13}$ cm⁻³, $f_{pe}/f_{ce}=3-10$). The core plasma is overdense to emission for the first ~ 10 cyclotron harmonics. Thermal EBW emission can occur at these cyclotron resonances; the EBW is strongly absorbed [2, 3, 14] in the shaded region between the cyclotron frequency and the upper-hybrid frequency ($f_{UH} = (f_{pe}^2 + f_{ce}^2)^{1/2}$) when the wave frequency (f) equals nf_{ce} , where harmonic

number $n=1, 2, 3, \dots$. In this region, f_{UH} is dominated by the f_{pe} contribution, and so has the shape of the plasma density profile. f_{pe} falls off quickly in the scrape-off layer (SOL) due to the presence of a limiter, as will be discussed.

Mode conversion of the emitted, radially outgoing EBW to X-mode waves can occur at the layer where $f=f_{UH}$. Outboard of the upper-hybrid layer, these X-mode waves will not be strongly absorbed. X-mode waves can only encounter the first few f_{ce} harmonics in the underdense region of the SOL ($R>58$ cm) where $T_e\sim 15$ eV and $n_e\sim 10^{12}$ cm⁻³ are too low to allow strong absorption [1]. Further inboard, the harmonic number is too high to allow the X-mode to be absorbed; electromagnetic cyclotron-resonant absorption decreases with increasing harmonic number. Thus, the upper-hybrid layer forms a natural boundary between the optically thick plasma (shaded) in which ECE power is carried by the EBW and optically thin plasma (unshaded) in which the emission has converted to the undamped X-mode.

As discussed in Reference 11, discrete transitions are expected between emission at different harmonics as the radiometer frequency is increased. A radiometer tuned to a frequency f viewing the plasma from the low-field side looks through the plasma until the first optically thick cyclotron resonance is encountered, i.e. the furthest outboard location where $f=nf_{ce}$ in the shaded region. The blackbody T_{rad} measured will be T_e at that location, reduced by the finite mode conversion fraction. As f is increased, a harmonic overlap will occur when the next cyclotron harmonic ($n+1$) crosses into the shaded region and becomes optically thick. This transition occurs where that cyclotron harmonic curve crosses f_{UH} in Figure 1. Just above that frequency, the EBW emission layer jumps out to the location where $f=f_{UH}$, and T_{rad} will thus generally drop. Increasing f further, the emission layer moves inward again, and T_{rad} increases. As depicted in Reference 11, the $T_{rad}(f)$ spectrum will have a sawtooth character, with discrete transitions

between emission at increasing harmonic numbers occurring for frequencies where $f_{UH} = n f_{ce}$ in Figure 1. This feature was observed in this work, as will be presented in section IV, and was previously reported on the Mega Amp Spherical Tokamak [15].

III. THE CDX-U EBW DIAGNOSTIC INSTRUMENT

EBW emission via B-X mode conversion has been studied in the CDX-U ST with an instrument that combines an in-vacuum quad-ridged horn antenna, a local limiter, and a Langmuir probe array as shown in Figure 2 [16]. The antenna views the plasma radially from the outboard side of the plasma near the midplane, and is oriented perpendicular to the magnetic field in order to couple to rays with no index of refraction vector component along the direction of the field ($n_{\parallel}=0$). B-X mode conversion efficiency for $n_{\parallel}=0$ is given by [4]

$$C = C_{max} \cos^2(\phi/2 + \theta) \quad (1)$$

where $\cos^2(\phi/2 + \theta)$ is a factor relating to the phasing of the waves in the mode conversion region [4, 17]. The maximum mode conversion efficiency (C_{max}) is given by

$$C_{max} = 4e^{-\pi\eta}(1 - e^{-\pi\eta}) \quad (2)$$

and depends sensitively on the electron density scale length ($L_n = |n_e / (dn_e/dR)|$) at the mode conversion layer. When the magnetic scale length in the mode conversion region $L_B \gg L_n$ as in CDX-U,

$$\eta \approx (2\pi f_{ce} L_n / (c \alpha)) ((1 + \alpha^2)^{1/2} - 1)^{1/2} \quad (3)$$

where f_{ce} , L_n , and $\alpha = f_{pe}/f_{ce}$ are evaluated at the upper-hybrid resonance layer where the B-X conversion occurs. Obtaining $C \sim 100\%$, or equivalently radiation temperature $T_{rad} \sim T_e$, requires $L_n \approx 0.5$ cm in CDX-U.

The mode conversion layer for emission at the first two f_{ce} harmonics lies in the SOL in CDX-U. It is possible to place material objects in this region of cold plasma, and so the graphite local limiter is used to shorten L_n to the value theoretically required to optimize C and produce mode conversion efficiencies near 100%. The plasma equilibrium is not perturbed by this structure, as it is not the primary limiter at the last closed flux surface (LCFS). The Langmuir probe array is used to measure the resulting L_n , and T_{rad} was found to agree well with T_e (measured separately by Thomson scattering) when $L_n \sim 0.5$ cm, in good agreement with theory [6]. However, attaining high mode conversion is not critical to the measurements of EBW harmonic overlap discussed here. The B-X mode conversion efficiency must be adequate to resolve the discrete transitions expected in the emitted spectrum, but an absolute measurement of T_e is not required in order to obtain magnetic field profile information.

IV. EXPERIMENTAL OBSERVATION OF EBW HARMONIC OVERLAP IN CDX-U

The discrete transitions described above have been measured in CDX-U using the 4-8 GHz and 8-12 GHz radiometers, each swept over its full frequency range every 0.1 ms with T_{rad} sampled at 3 Mhz [18]. For this experiment, both local limiters were extended with the antenna positioned near the LCFS as in Figure 2. The spectrum of B-X mode converted EBW emission shown in Figure 3 is obtained. Three radiometer scans from the 65 kA plasma current peak of the discharge are shown for each radiometer (black and gray). The T_{rad} fluctuation is due to L_n fluctuation affecting the mode conversion efficiency and possibly also refractive effects that change the EBW emission location in the plasma [6, 16]. Since C remains above 50% and refractive effects change the effective T_e but do not affect the mode conversion process at the

plasma edge, we are able to identify unambiguously the harmonic transition frequencies. The first two harmonic transitions are indicated by dashed vertical lines, with hatched regions indicating the radiometer bandwidth. These frequencies are characterized by the sudden drop in T_{rad} with low T_{rad} on the high-frequency side of the transition, where the emission is originating from near the upper-hybrid resonance layer at the cold plasma edge.

Using $n_e(R)$ from Langmuir probe measurements and $B(R)$ from EFIT modeling, we can explore the theoretical prediction that these harmonic transition frequencies occur at overlaps in $f_{UH}(R)$ and $nf_{ce}(R)$. Figure 4 shows the cyclotron harmonic and upper-hybrid frequency profiles in the CDX-U SOL. The cyclotron frequency is calculated with magnetic equilibria from EFIT calculations in which the plasma boundary and toroidal current were fixed, and Langmuir probe array measurements are averaged over the time window of Figure 3 to calculate the average f_{UH} (diamonds). The shaded region in Figure 4 indicates the worst-case error bars in f_{UH} , including fast n_e fluctuation and 35% probe error, which contribute on comparable levels. Also plotted are the harmonic transition frequencies measured in Figure 3 (dashed horizontal lines in Figure 4). The overlap between f_{UH} and the f_{ce} harmonics (open circles) agree with the measured transition frequencies within the radiometer bandwidth (hatched regions) as well as within the error in f_{UH} .

The information gained in this experiment can be viewed in several ways. First, it is a validation of the hot-plasma wave theory that determines the physics of the EBW. The data supports theoretical predictions that the EBW is strongly absorbed at the electron cyclotron harmonics beneath f_{UH} with high localization, even at plasma parameters as modest as $T_e \sim 15$ eV, $n_e \sim 10^{12}$ cm⁻³ in the CDX-U SOL. Second, we may consider this measurement to be a corroboration of the EFIT modeling used in the calculations, as the value of $|B|$ at the upper-

hybrid layer is constrained to within a few percent by the comparison of Figure 4. Finally, this experiment supports the q profile diagnostic scheme proposed in Reference 11.

V. DISCUSSION OF MAGNETIC FIELD PROFILE DIAGNOSTIC IMPLEMENTATION

Direct measurement of the magnetic field profile is presently a challenge in fusion plasmas, as difficult spectroscopic measurements are required to infer $B(R)$ from motional Stark shift of spectral lines of particles in a diagnostic neutral beam [19]. The EBW harmonic transition frequencies are related both to $n_e(R)$ and $B(R)$, so that knowledge of one allows calculation of the other at the points where the harmonic transitions occur. Magnetic field profile measurements via EBW harmonic overlap observation would require an independently measured $n_e(R)$ to be combined with an initial guess for $B(R)$, for example n_e from Thomson scattering measurements and B from EFIT reconstruction. Derived in Reference 11 by imposing the condition $f_{UH} = nf_{ce} = f_n$ at the measured harmonic overlap frequencies f_n , the relations

$$n_e(R_n) = \frac{2\pi\epsilon_0 m_e}{e^2} \left(1 - \frac{1}{n^2}\right) f_n^2 \quad (4)$$

$$B(R_n) = \frac{2\pi m_e}{e} \frac{f_n}{n} \quad (5)$$

can be used to reconstruct the magnetic field profile, where R_n is the major radial location at which the electron cyclotron harmonic and upper-hybrid frequency coincide. First, the initial guess for $B(R)$ is needed to identify the harmonic number $n = 2, 3, 4, \dots$ corresponding to each observed harmonic overlap frequency f_n . Then, the independently measured electron density profile is interpolated in equation (4) to determine R_n . Finally, the magnitude of the magnetic field at R_n is determined from equation (5). In this way, a set of discrete $B(R)$ points are

obtained, with error in B resulting from experimental resolution of the harmonic overlap frequencies, and error in R from the quality of both the f_n and $n_e(R)$ measurements. The $|B|$ profile obtained in this manner would aid in determining the q profile.

Using B-X mode conversion to measure harmonic overlap frequencies could be challenging at higher harmonics, as the longer L_n and correspondingly thicker f_R-f_{UH} X-mode tunneling region (see Figure 1) would lead to a reduced B-X emission signal. If the conversion efficiency were too small and the conversion region far from the antenna, the harmonic overlap transition might be dominated by reflected waves bouncing between the vessel wall and the cutoff layer. The B-X-O process can in theory always provide 100% conversion efficiency with proper choice of $n_{||}$, and might be a better choice for observation of high-harmonic overlap. In practice, however, the signal could be affected by frequency dependence in the oblique angular window of conversion, which would change as the plasma parameters at the mode conversion layer and the shape and location of the layer itself varied. An added complication for either approach is that $B(R)$ near the magnetic axis may not be as well constrained, since few $f_{UH}=nf_{ce}$ overlaps occur at spatial locations near the plasma core (Figure 1). Furthermore, this technique allows measurement of the magnetic field profile only outboard of the magnetic axis.

A broadband radiometer is required to implement the above technique. Attractive features of measuring $B(R)$ via the harmonic transition frequencies, are that the radiometers need not be calibrated and the frequency measurement can be performed with high precision. With a calibrated radiometer, though, $T_{rad}(R)$ could be obtained outboard of the plasma core by associating T_{rad} just above the n^{th} harmonic overlap frequency with R_n inferred at that position [11]. This would provide a discrete set of $T_{rad}(R)$ points without the need for EBW ray-tracing in order to associate radiometer detection frequency with an EBW emission location [6, 16].

NSTX equilibria with $\beta = 40\%$ [20] are marked by the presence of a non-monotonic magnetic field profile with a dip in $B(R)$ near the center of the plasma, as seen in the nf_{ce} profiles of Figure 5. Here the magnetic axis is located at a major radius of $R_M = 1.2$ m, the last closed flux surface at 1.55 m, and a density scale length of 1 cm is assumed in the scrape-off layer. The “magnetic well” masks EBW emission from the plasma core at lower harmonics, and may lead to additional discrete transitions in the EBW emission spectrum corresponding to the jump in the emission across the well from the low-field to the high-field side of the plasma as frequency is increased. Bold lines in Figure 5 indicate the spatial origin of EBW emission capable of propagating radially outward to the upper-hybrid layer without encountering an absorbing cyclotron resonance. Horizontal dotted lines indicate frequencies at which a discrete transition would be expected in the B-X converted spectrum. In addition to the $f_{UH} = nf_{ce}$ harmonic overlap frequencies, there are transition frequencies corresponding to reabsorption of high-field side EBW emission by the m^{th} electron cyclotron at the minimum of the magnetic well. These may be used to measure the value of $|B|$ at the magnetic axis by equating the measured transition frequency $f_m = mf_{ce}(R_M)$, where in this example $m = 2, 3, 7,$ and 8 (from Figure 5). The challenge in this scenario would likely be in identifying the harmonic numbers n and m for each transition frequency observed in the EBW spectrum.

Interestingly, the upper-hybrid profile can overlap the nf_{ce} profiles in the magnetic well region, as seen in Figure 5. This would allow the study of EBW emission from the high-field side of a cyclotron resonance (bold lines outboard of the magnetic axis). This geometry is relevant to toroidal plasmas such as the field-reversed configuration (FRC) in which $B(R)$ increases with R , and experiments in a suitably high- β ST could determine if EBW techniques could be applied to such plasmas. EBW theory in the $n_{\parallel} = 0$ limit [13] predicts a thin evanescent region on the high-

field side of the nf_{ce} resonances through which emitted waves would have to tunnel in order to reach the outboard upper-hybrid mode conversion layer. This could result in suppressed emission in frequency bands for which the magnetic field is increasing with R at the nominal emission location. Ray-tracing including finite- n_{\parallel} effects for a real antenna geometry is necessary in order to shed further light on this process.

VI. CONCLUSIONS

Discrete transitions in the EBW emission spectrum in CDX-U have been measured corresponding to the first two harmonic overlaps. A sudden drop in T_{rad} with increasing emission frequency is discernable despite fluctuating mode conversion efficiency. These frequencies agree within errors with the harmonic overlaps calculated from f_{UH} and nf_{ce} profiles using $B(R)$ modeled with EFIT and $n_e(R)$ measured with a Langmuir probe array. These data validate the EBW physics predicted by plasma wave theory, including strong absorption at (and thermal emission from) electron cyclotron harmonic resonances and transfer of energy to undamped electromagnetic waves at the mode conversion layer spanning the upper-hybrid resonance.

The results presented here support the q profile measurement technique proposed in Reference 11. As the EBW harmonic overlap frequencies are uniquely determined by $n_e(R)$ and $B(R)$, the magnetic field profile in an ST could be measured by observing this feature of the emitted spectrum while measuring the density profile independently. Such a measurement would require a broadband radiometer set extending from the edge electron cyclotron frequency to the core

plasma frequency of the machine. Observation of the first two harmonic overlap frequencies provided a measurement of $|B|$ in the CDX-U SOL with accuracy of a few percent.

ACKNOWLEDGEMENTS

The authors would like to thank J. Taylor, R. Majeski, R. Kaita and the CDX-U team for their contributions to this research, F. Paoletti for his help with EFIT, and E. Yu for valuable discussion. This work was supported by U.S. Department of Energy Contract DE-AC02-76-CHO-3073 as part of the “Innovations in Magnetic Fusion Energy Diagnostic Systems” program.

- [1] M. Bornatici, R. Cano, O. De Barbieri, and F. Engelmann, *Nucl. Fusion* **23**, 1153 (1983).
- [2] P. C. Efthimion, J. C. Hosea, R. Kaita, R. Majeski, and G. Taylor, *Rev. Sci. Instrum.* **70**, 1018 (1999).
- [3] J. Hosea, V. Arunasalam, and R. Cano, *Phys. Rev. Lett.* **39**, 408 (1977).
- [4] A. K. Ram and S. D. Schultz, *Phys. Plasmas* **7**, 4084 (2000).
- [5] J. Preinhaelter and V. Kopecky, *J. Plasma Phys.* **10**, 1 (1973).
- [6] B. Jones, P. Efthimion, G. Taylor *et al.*, *Phys. Phys. Rev. Lett.* **90**, 165001 (2003).
- [7] G. Taylor, P. C. Efthimion, B. Jones, B. P. LeBlanc, and R. Maingi, *Phys. Plasmas* **9**, 167 (2002).
- [8] P. K. Chattopadhyay, J. K. Anderson, T. M. Biewer, D. Craig, C. B. Forest, R. W. Harvey, and A. P. Smirnov, *Phys. Plasmas* **9**, 752 (2002).
- [9] H. P. Laqua, H. J. Hartfuß, and W7-AS Team, *Phys. Rev. Lett.* **81**, 2060 (1998).
- [10] H. P. Laqua, V. Erckmann, H. J. Hartfuß, H. Laqua, W7-AS Team and ECRH Group, *Phys. Rev. Lett.* **78**, 3467 (1997).
- [11] V. F. Shevchenko, *Plasma Phys. Reports* **26**, 1000 (2000).
- [12] L. L. Lao, H. St. John, R. D. Stambaugh, A. G. Kellman, and W. Pfeiffer, *Nucl. Fusion* **25**, 1611 (1985).
- [13] T. Stix, *Waves in Plasmas*. Springer-Verlag, New York (1992).
- [14] M. Bornatici, C. Maroli, and V. Petrillo, *Proceedings of the 3rd Joint Varenna-Grenoble International Symposium on Heating in Toroidal Plasmas*, Grenoble, 1982, edited by C. Gomezano, G. G. Leotta, and E. Sindoni (Pergamon Press, New York, 1982), Vol. 2, p. 691.
- [15] V. Shevchenko, G. Cunningham, and S. Field, *Proceedings of the 28th EPS Conference on Controlled Fusion and Plasma Physics*, Funchal, 2001, edited by C. Silva, C. Varandas, and D. Campbell (European Physical Society, Mulhouse Cedex, 2001), ECA Vol. 25A, p. 1285.
- [16] B. Jones, Ph.D. thesis, Princeton University, 2002.
- [17] A. K. Ram, A. Bers, and S. D. Schultz, *Phys. Plasmas* **3**, 1976 (1996).
- [18] G. Taylor, P. Efthimion, B. Jones, T. Munsat, J. Spaleta, J. Hosea, R. Kaita, R. Majeski, and J. Menard, *Rev. Sci. Instrum.* **72**, 285 (2001).
- [19] F. M. Levinton, *Rev. Sci. Instrum.* **70**, 810 (1999).
- [20] J. Menard, *Nucl. Fusion* **37**, 595 (1997).

FIG. 1. Characteristic frequencies relevant to EBW emission and mode conversion processes for nominal CDX-U plasma parameters. The plasma is optically thick to EBWs at frequencies nf_{ce} in the shaded region.

FIG. 2. The CDX-U EBW diagnostic combines a quad-ridged horn antenna to measure emission, a movable local limiter (half shown) to modify L_n in front of the antenna to optimize mode conversion, and a Langmuir probe array to measure L_n .

FIG. 3. The EBW emission spectrum during three 0.1 ms scans of the 4-8 GHz (black) and 8-12 GHz (gray) CDX-U radiometers. The first two harmonic overlap frequencies are observed (dashed lines) with the radiometer bandwidth indicated (hatched regions).

FIG. 4. Characteristic frequencies in the CDX-U SOL. The measured harmonic overlap frequencies (dashed horizontal lines, radiometer bandwidth shown hatched) from Fig. 3 agree with the expected overlap between nf_{ce} and f_{UH} (open circles). Error in f_{UH} (shaded region) is due to 35% n_e error from Langmuir probes and n_e fluctuations over the time window of Fig. 3.

FIG. 5. Characteristic frequencies for a $\beta=40\%$ NSTX equilibrium. The bold lines indicate regions of space from which thermal EBWs of a given frequency nominally originate. Dotted horizontal lines show frequencies at which transitions in the emission spectrum are expected.

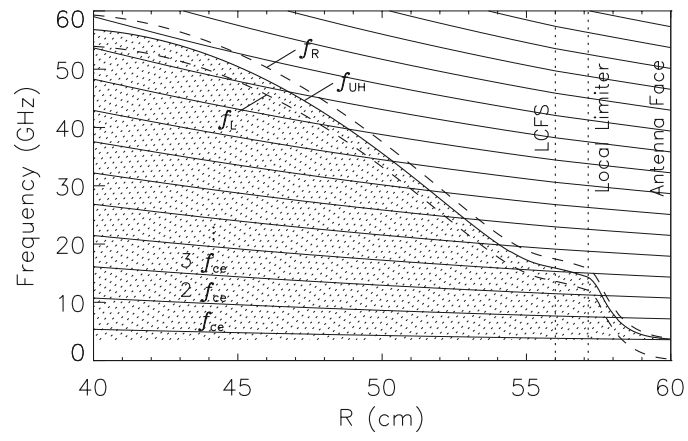


FIGURE 1, B. Jones

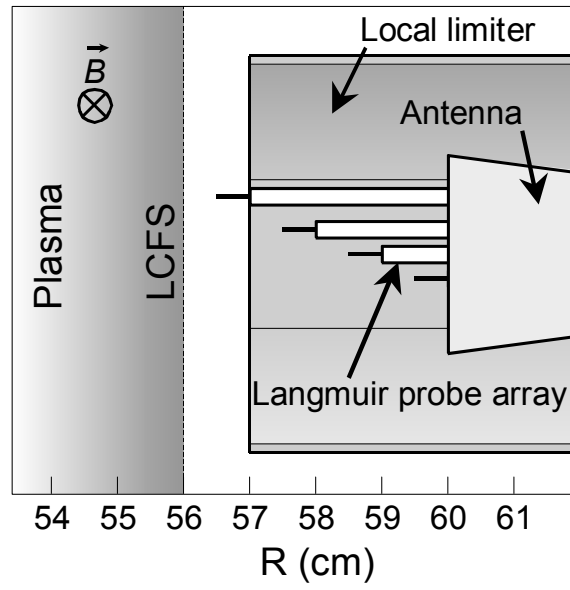


FIGURE 2, B. Jones

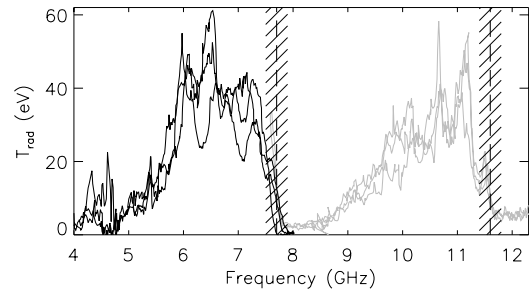


FIGURE 3, B. Jones

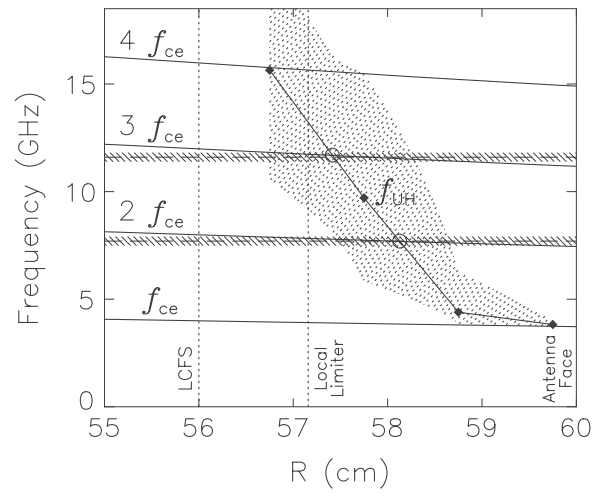


FIGURE 4, B. Jones

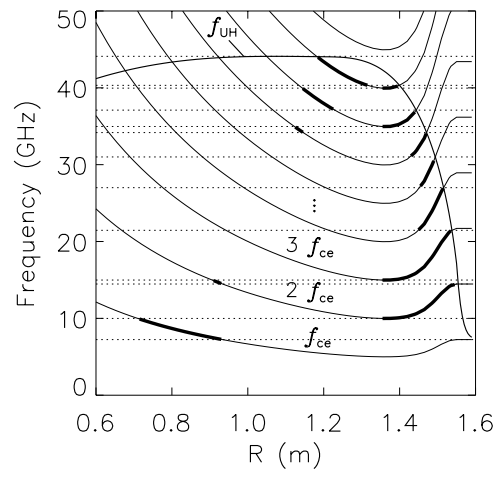


FIGURE 5, B. Jones

External Distribution

Plasma Research Laboratory, Australian National University, Australia
Professor I.R. Jones, Flinders University, Australia
Professor João Canalle, Instituto de Fisica DEQ/IF - UERJ, Brazil
Mr. Gerson O. Ludwig, Instituto Nacional de Pesquisas, Brazil
Dr. P.H. Sakanaka, Instituto Fisica, Brazil
The Librarian, Culham Laboratory, England
Mrs. S.A. Hutchinson, JET Library, England
Professor M.N. Bussac, Ecole Polytechnique, France
Librarian, Max-Planck-Institut für Plasmaphysik, Germany
Jolan Moldvai, Reports Library, Hungarian Academy of Sciences, Central Research Institute
for Physics, Hungary
Dr. P. Kaw, Institute for Plasma Research, India
Ms. P.J. Pathak, Librarian, Institute for Plasma Research, India
Ms. Clelia De Palo, Associazione EURATOM-ENEA, Italy
Dr. G. Grosso, Instituto di Fisica del Plasma, Italy
Librarian, Naka Fusion Research Establishment, JAERI, Japan
Library, Laboratory for Complex Energy Processes, Institute for Advanced Study,
Kyoto University, Japan
Research Information Center, National Institute for Fusion Science, Japan
Dr. O. Mitarai, Kyushu Tokai University, Japan
Dr. Jiengang Li, Institute of Plasma Physics, Chinese Academy of Sciences,
People's Republic of China
Professor Yuping Huo, School of Physical Science and Technology, People's Republic of China
Library, Academia Sinica, Institute of Plasma Physics, People's Republic of China
Librarian, Institute of Physics, Chinese Academy of Sciences, People's Republic of China
Dr. S. Mirnov, TRINITI, Troitsk, Russian Federation, Russia
Dr. V.S. Strelkov, Kurchatov Institute, Russian Federation, Russia
Professor Peter Lukac, Katedra Fyziky Plazmy MFF UK, Mlynska dolina F-2,
Komenskeho Univerzita, SK-842 15 Bratislava, Slovakia
Dr. G.S. Lee, Korea Basic Science Institute, South Korea
Institute for Plasma Research, University of Maryland, USA
Librarian, Fusion Energy Division, Oak Ridge National Laboratory, USA
Librarian, Institute of Fusion Studies, University of Texas, USA
Librarian, Magnetic Fusion Program, Lawrence Livermore National Laboratory, USA
Library, General Atomics, USA
Plasma Physics Group, Fusion Energy Research Program, University of California
at San Diego, USA
Plasma Physics Library, Columbia University, USA
Alkesh Punjabi, Center for Fusion Research and Training, Hampton University, USA
Dr. W.M. Stacey, Fusion Research Center, Georgia Institute of Technology, USA
Dr. John Willis, U.S. Department of Energy, Office of Fusion Energy Sciences, USA
Mr. Paul H. Wright, Indianapolis, Indiana, USA

The Princeton Plasma Physics Laboratory is operated
by Princeton University under contract
with the U.S. Department of Energy.

Information Services
Princeton Plasma Physics Laboratory
P.O. Box 451
Princeton, NJ 08543

Phone: 609-243-2750
Fax: 609-243-2751
e-mail: pppl_info@pppl.gov
Internet Address: <http://www.pppl.gov>